Seismic Performance of RC Frame Having Different Wall Thickness

[1] Haran Pragalath D C, [2] Sivakumar Ramalingam, [3] Harry Wichers

[1]Assistant Professor, British Applied College, Umm Al Quwain, United Arab Emirates.
[2]Professor, British Applied College, Umm Al Quwain, United Arab Emirates.
[3]Professor, British Applied College, Umm Al Quwain, United Arab Emirates
Corresponding Author: Haran Pragalath D C

Abstract: *This paper presents the performance comparison of bare frames, fully and partial infilled frames having different infill wall thickness in a probabilistic frame work. Normally at design stage of buildings, infill walls are considered as non-load bearing walls due to more uncertainties involved in the modelling of masonry infill walls, whereas it can resist significant amount of lateral forces under seismic loads which may change the global performance of buildings. In this study exceedance probabilities and the reliability index of RC frames with two different infill wall thicknesses used in the Indian Construction practice are computed. It is found that higher thickness of infill wall is beneficial to the global performance of buildings for a fully infilled frame and detrimental for partially infilled frames.*
Keywords: *Equivalent Strut, Peak Ground Acceleration, Fragility curves, Reliability Index derivatives.*

I. INTRODUCTION

Generally, in reinforced concrete framed structures, infill walls are used as non-structural partition walls. During design stage of such framed structure, stiffness and strength of infill walls are ignored considering only the mass. Past earthquakes demonstrated that these non-structural elements had beneficial effects on the lateral capacity of the building in case of fully-infilled frames. Later it is found that, it may give detrimental behaviour to partially infilled frames. This beneficial and detrimental effects on infilled frames are mostly depends upon many parameters of infill walls such as, infill material strength, thickness of wall, type of infill etc. Among this, thickness of wall plays a major role as the change in thickness alters the infill wall strength significantly. The in-situ thickness of infill walls are generally decided by several functional and architectural reasons. The two commonly adopted thickness values of the infill walls in Indian construction practice are 115mm and 230mm. Many studies have been reported on the effects of infill walls in the global performance of RC framed buildings, no study has been reported on how far the thickness of an infill wall can alter the global performance of buildings in a probabilistic framework. The present study is focussed on the evaluation of seismic performance of typical RC infilled frames designed as per Indian standards considering different infill wall thicknesses through the fragility curves and corresponding reliability index values.

II. STUDIES ON INFILLED FRAMES

Several experimental studies (Polyakov (1960), Holmes (1961), Stafford-Smith (1962), Mainstone and Week (1970), Mainstone (1971), Mehrabi et al. (1996), Al-Chaar (2002), Kaltakci et al. (2008)) on infilled frames have been carried out and reported that behaviour of infilled frames are quite different from the bare frames. These studies were focussed on the formulation of equivalent diagonal strut to model the infill walls. Buonopane and White (1999) observed the formation of compressive struts at low force levels. Lee and Woo (2002) performed dynamic and static monotonic tests on a 1/5-scale two-bay three-story masonry infilled non-ductile concrete frame and concluded that the large increase in stiffness, strength, and inertial force (due to added mass) of the infilled frame compared to the bare frame. Hashemi and Mosalam (2006) conducted a shake-table test on a 3/4-scale one-bay masonry infilled concrete frame that represents a substructure of a five-story prototype. Observations showed the same results as previous tests in the behaviour of the infilled frame. Anil and Altin (2007) conducted cyclic tests on nine 1/3-scale one-bay, one-story partially infilled ductile RC frames with different configurations and locations of the openings. It is reported that the fully infilled frame has seven times greater energy dissipation capacity than the bare frame.

III. METHODOLOGY

The methodology adopted in the present study is to evaluate the seismic risk of buildings in terms of fragility curves and reliability indices. An accepted simplified method (Ellingwood, 2001) for the development of fragility curves is adopted in the present study. The methodology reported by Ellingwood (2001) for estimation of seismic risk involves three parts. First part is the identification of the seismic hazard, P [A = a], described by the annual probabilities of specific levels of earthquake motion. The seismic hazard at a site is usually represented through a seismic hazard curve, GA(x) which is a plot of P [A = a] versus the level of earthquake motion (a) expressed in terms. Second part is the analysis of global response of the structural system. The response analysis of the structure is carried out by conducting nonlinear time history analyses for different earthquakes, and the response is expressed in terms of maximum inter- storey drift at any storey. Third part is the calculation of limit state probabilities of attaining a series of (increasingly severe) limit states, LSi, through the expression:

$$P\left[LS_i\right] = \sum_a P\left[LS_i \mid A = a\right]P\left[A = a\right]$$
(1)

The conditional probability is denoted as the seismic fragility, FR(x). This conditional probability, explicitly stated, is the probability of meeting or exceeding a specified level of damage, LS, given a ground motion which has a certain level of intensity, a. This conditional probability is often assumed to follow a two parameter lognormal probability distribution (Cornell et al. 2002, Song and Ellingwood, 1999).

A point estimate of the limit state probability of state i can be obtained by convolving the fragility FR(x) with the derivative of the seismic hazard curve, GA(x), thus removing the conditioning on acceleration as per Eq. (1).

$$P\left[LS_i\right] = \int F_R\left(x\right)\frac{dG_A}{dx}\,dx$$
(2)

The parameters of the fragility-hazard interface must be dimensionally consistent for the probability estimate to be meaningful. The reliability index corresponding to the probability of failure can be found by the following standard equation as shown below.

$$\beta_{Pf} = -\phi^{-1}\left(P\left[LS_i\right]\right)$$
(3)

Where ϕ ( ) represents the standard normal distribution.

3.1 Seismic Hazard Analysis

The seismic hazard (GA) at a site is expressed through a complementary cumulative distribution function (CCDF). The hazard function is the annual frequency of motion intensity at or above a given level (x). Elementary seismic hazard analysis shows that at moderate to large values of ground acceleration, there is a logarithmic linear relation between annual maximum earthquake ground or spectral acceleration, and the probability, GA(a), that specific values of acceleration are exceeded. This relationship implies that A is described by following equation suggested by Ellingwood (2001),

$$G_A\left(x\right) = 1 - \exp[-\left(x/u\right)^{-k}]$$
(4)

u and k are parameters of the distribution. Parameter k defines the slope of the hazard curve which, in turn, is related to the coefficient of variation (COV) in annual maximum peak ground acceleration.
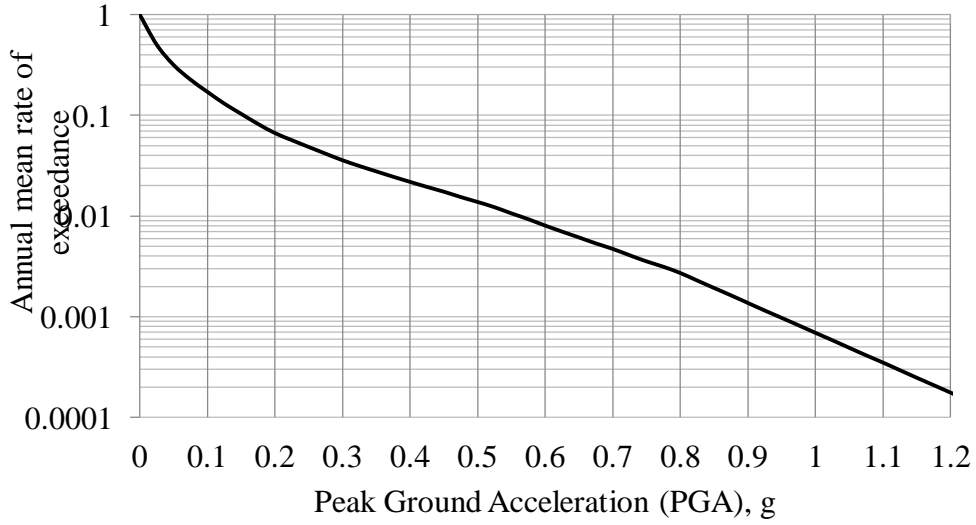
The seismic hazard curve of north-east region of India (Manipur), which is one of the most seismically active regions, developed by Pallav et al. (2012) as shown in Fig. 1. This hazard curve is selected in the present study for estimation of risk. The annual frequency of being exceedance of PGA for about 475 years return period (10% exceedance probability in 50 years, Design Basis Earthquake, DBE) and about 2500 year return period (2% exceedance probability in 50 years, Maximum Considered Earthquake, MCE) for Manipur Region is found to be 0.83g and 1.08g respectively.

3.2 Development of Fragility Curves.

The fragility function represents the probability of exceedance of a selected Engineering Demand Parameter (EDP) for a selected structural limit state (LS) for a specific ground motion intensity measure (IM). Fragility curves are cumulative probability distributions that indicate the probability that a component/system will be damaged to a given damage state or a more severe one, as a function of a particular demand. The seismic fragility, FR(x) can be expressed in closed form using the following equation,

$$P\left(D \geq C \mid IM\right) = \phi\left(\frac{\ln\dfrac{S_D}{S_C}}{\sqrt{\beta_{D\mid IM}^2 + \beta_c^2}}\right)$$
(5)

where, D is the drift demand, C is the drift capacity at chosen limit state, SD and SC are the median of the demand and the chosen limit state (LS) respectively. βd/IM and βc are dispersions in the intensity measure and capacities respectively. A fragility curve can be obtained for each limit state.

Fig.1. Seismic hazard curves of North East region, India (Pallav et al., 2012).

3.3 Development of Fragility Curves.

The fragility function represents the probability of exceedance of a selected Engineering Demand Parameter (EDP) for a selected structural limit state (LS) for a specific ground motion intensity measure (IM). Fragility curves are cumulative probability distributions that indicate the probability that a component/system will be damaged to a given damage state or a more severe one, as a function of a particular demand. The seismic fragility, FR(x) can be expressed in closed form using the following equation,

$$P(D \geq C \mid IM) = \phi \left(\frac{\ln \dfrac{S_D}{S_C}}{\sqrt{\beta_{D|IM}^2 + \beta_c^2}} \right)$$

(5)

where, D is the drift demand, C is the drift capacity at chosen limit state, SD and SC are the median of the demand and the chosen limit state (LS) respectively. βd/IM and βc are dispersions in the intensity measure and capacities respectively. A fragility curve can be obtained for each limit state.

The seismic demand is usually described through probabilistic seismic demand models (PSDMs) particularly for nonlinear time history analyses which are given in terms of an appropriate intensity measure (IM). It has been suggested by Cornell et al. (2002) that the estimate of the median demand, EDP (SD) can be represented in a generalized form by a power model as given in Eq. 6.

$$EDP = a(IM)^b$$

(6)

Where, a and b are the regression coefficients of the Probabilistic Seismic Demand Model (PSDM). Eq. 5 can be rewritten for system fragilities (Nielson [17]) as follows:

$$P(D \geq C \mid IM) = \phi \left(\frac{\ln IM - \ln IM_m}{\beta_{comp}} \right)$$

(7)

where, $IM_m = \exp \left(\dfrac{\ln S_C - \ln a}{b} \right)$, and the dispersion component, βcomp is given as

$$\beta_{comp} = \frac{\sqrt{\beta_{D|IM}^2 + \beta_c^2}}{b}$$

(8)

The dispersion βD/IM on the inter-storey drifts (di) from the time history analysis can be calculated using Eq. 9 where a(IM)b is the best-fit line that represents the mean.

$$\beta_{D|IM} \cong \sqrt{\frac{\sum \left[\ln(d_i) - \ln(aIM^b) \right]^2}{N-2}}$$

(9)

The dispersion in capacity, β_c is dependent on the building type and construction quality. ATC 58 (2012) suggests values of βc as 0.10, 0.25 and 0.40 depending on the quality of construction good, fair and poor respectively. In this study, dispersion in capacity has been assumed as 0.25, as shown in Table 2. The methodology adopted in this study has been used by many researchers Nielson, (2005), Rajeev and Tesfamariam (2012), Davis et al. (2010), Haran et al, 2015b, Avinash et. al. 2017) in past to develop fragility curves of RC structures.

3.4 Performance limit states

Limit states define the capacity of the structure to withstand different levels of damage. The median inter-storey drift limit states for both RC moment resisting infilled and bare frame structures defining the capacity of the structure at various performance levels (SC) are suggested by Ghobarah (2000) and ASCE/SEI 41-06 (2007). Drift limits for RC frames as per ASCE/SEI 41-06 (2007) as shown in the Table 1 for different limit states: light repairable damage (IO), moderate repairable damage (LS) and near collapse (CP) are considered in the present study.

Table 1: Damage limits and dispersion associated with various structural performance levels

Limit states designation	Performance levels	Median Inter-storey Drifts Sc for Concrete frames, (%) (ASCE/SEI 41-06 [22])	Dispersion, βc (ATC 58 [18])
O	Light repairable damage	1	0.25
LS	Moderate repairable damage	2	0.25
CP	Near collapse	4	0.25

IV. FRAMES CONSIDERED

The building frame considered for numerical analysis in the present study is designed for the highest seismic zone (zone V with PGA of 0.36g) as per Indian standard IS 1893 (2002) considering medium soil conditions (N-value 10 to 30). The characteristic strength of concrete and steel are taken as 25MPa and 415MPa respectively. The buildings are assumed to be symmetric in plan, and hence a single plane frame is considered to be representative of the building along one direction. Typical bay width and column height in this study are selected as 5m and 3.2m respectively, as observed from the study of typical existing residential buildings. A configuration of four storeys and two bays is considered. The dead load of the slab (5 m × 5 m panel) including floor finishes is taken as 3.75 kN/m2 and live load as 3 kN/m2. The design base shear (VB) is calculated as per equivalent static method (IS 1893, 2002). The structural analysis for all the vertical and lateral loads is carried out by ignoring the infill wall strength and stiffness (conventional). The design of the RC elements are carried out as per IS 456 (2000) and detailed as per IS 13920 (1993). Bare frame (BF), Fully infilled frame (FF) and Partially infilled frames are considered in the study as shown in Fig. 2. Tables 2 summarize the details of columns and beam sections of considered frame (Haran et.al. (2015a).
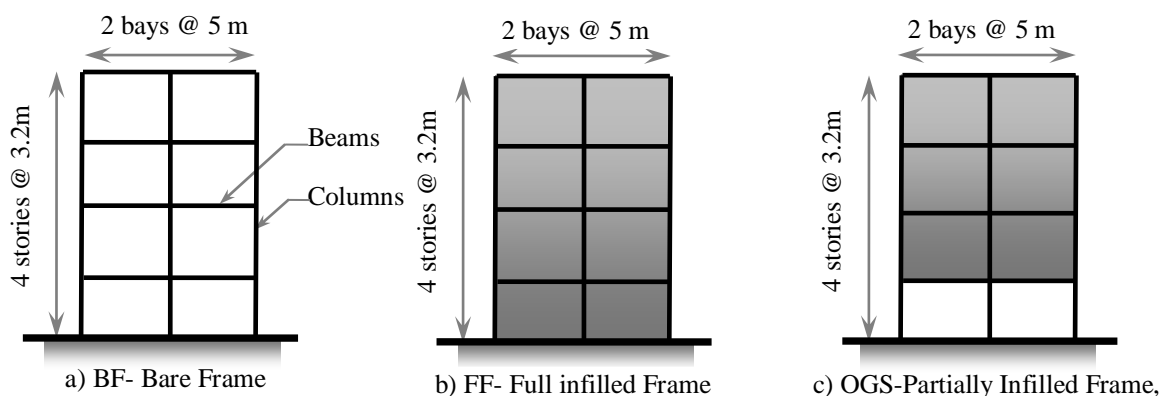
Fig. 2: Four storeyed RC frames considered in the study

V.   MODELING FOR NONLINEAR ANALYSIS

As per the methodology adopted, it is required to conduct a series of nonlinear dynamic time history analyses of all the selected frames. Opensees Laboratory tool developed by Frank et al. (2014) is used for the present study for nonlinear time history analyses. Force-based nonlinear beam-column element is used in the present study for modelling the beams and columns that consider the spread of plasticity along the element. Formulation of the fibre-based element is explained in Lee and Mosalam (2004). Sensitivity study conducted by Kunnath (2007) suggests five integration points for the fibre based element and hence five integration points are used in the present study.

Tables 2: Summarize the details of columns and beam sections of each frame.

Frame Section	Storey/level	Floor	Width (mm)	Depth (mm)	Reinforcement Details	
Column	Ground		350	350	8 - 20ϕ (uniformly distributed)	
	1-3		350	350	8 - 18ϕ (uniformly distributed)	
Beam	1,2		300	375	5 - 20 ϕ (top)	4 - 20ϕ (bottom)
	3		300	375	4 - 20ϕ (top)	3 - 20ϕ (bottom)
	4		300	325	4 - 20ϕ (top)	3 - 20ϕ (bottom)

VI. MODELING FOR NONLINEAR ANALYSIS

As per the methodology adopted, it is required to conduct a series of nonlinear dynamic time history analyses of all the selected frames. Opensees Laboratory tool developed by Frank et al. (2014) is used for the present study for nonlinear time history analyses. Force-based nonlinear beam-column element is used in the present study for modelling the beams and columns that consider the spread of plasticity along the element. Formulation of the fibre-based element is explained in Lee and Mosalam (2004). Sensitivity study conducted by Kunnath (2007) suggests five integration points for the fibre based element and hence five integration points are used in the present study.

6.1 Concrete and Steel Constitutive Models

Limit states define the capacity of the structure to withstand different levels of damage. The median inter-storey drift limit states for both RC moment resisting infilled and bare frame structures defining the capacity of the structure at various performance levels (SC) are suggested by Ghobarah [21] and ASCE/SEI 41-06 [22]. Drift limits for RC frames as per ASCE/SEI 41-06 [22] as shown in the Table 1 for different limit states: light repairable damage (IO), moderate repairable damage (LS) and near collapse (CP) are considered in the present study.

6.2 Infill Wall modelling

Many authors (Landi et al.(2012), Mosalam et al.(1997) , Al-Chaar (2002), Haran et. al (2015b) etc.) worked in the area of infill wall modelling and formulated a simple diagonal strut model which is numerically stable and computationally efficient. Different theories were proposed by many authors for determining the strength and stiffness of masonry infill walls. Dolsek and Fajfar (2008) has summarized and reviewed some of the works related to infill wall modelling. A recent infill wall model used by Celarec et al. (2012) developed by Panagiotakos and Fardis (1996) is considered in the present study. The first branch of the quadrilinear force-displacement envelope curve corresponds to the linear elastic behaviour up to the first cracking of the infill with a stiffness of

$$K_{el} = \frac{G_w A_w}{h_w}$$

(10)

where, A_w is the cross-sectional area of the infill panel, G_w is the elastic shear modulus of the infill material, and h_w is the clear height of the infill panel. The shear cracking strength is given by

$$F_{cr} = \tau_{cr} A_w$$

(11)

Where, τ_{cr} is the shear stress at cracking stage. The second branch of the envelope runs from the first cracking point up to the point of maximum strength, which is estimated as

$$F_{max} = 1.30 \cdot F_{cr}$$

(12)

The corresponding displacement is evaluated assuming secant stiffness up to the maximum strength, by Mainstone's (1971) formula, i.e. assuming an equivalent strut width equal to

$$b_w = 0.175 \left(\lambda_h h_w \right)^{-0.4} d_w \tag{13}$$

Where, dw is the clear diagonal length of the infill panel, and the coefficient λh is defined by the expression

$$\lambda_h = \sqrt{\frac{E_w t_w \sin(2\theta)}{4 E_c I_c h_w}} \tag{14}$$
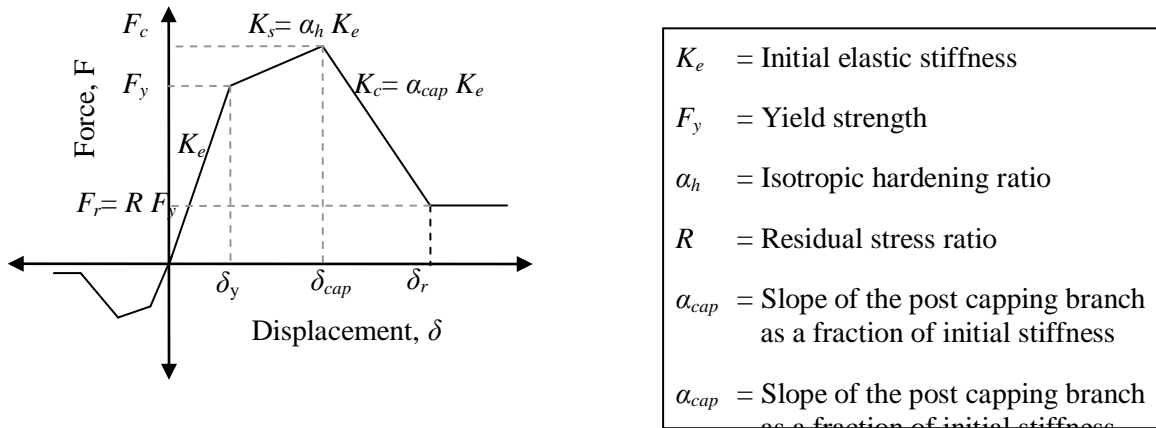
where Ew and Ec are the Young's modulus of the infill walls and of the RC frame, respectively, is the inclination of the diagonal with respect to horizontal plane, H and L are, respectively, the height and the length of the infill panel, tw is the thickness of the masonry infill and Ic is the moment of inertia of the RC column. Considering, Eqs. (14) & (15), the secant stiffness which targets the maximum strength of the infill can be calculated from the expression:

$$K_{sec} = \frac{E_w b_w t_w}{\sqrt{L^2 + H^2}} \cos^2 \theta \tag{15}$$

The third branch of the envelope is the post-capping degrading branch, which runs from the maximum strength to the residual strength. Its stiffness depends on the elastic stiffness, and is defined by means of the parameter α as:

$$K_{deg} = -\alpha \cdot K_{el} \tag{16}$$

Panagiotakos and Fardis(1996) has been suggested that 'α' should be within the range of values between 0.005 and 0.1, although the upper value corresponds to a brittle failure. In the the present study, α is assumed to have a value of 0.05 for all the masonry infills. The fourth branch of the envelope is the horizontal branch corresponding to the residual strength, which is conservatively assumed to be equal to 2% of the maximum strength. The typical quadrilinear force-displacement relationship of the diagonal struts (in compression), measured in the axial direction is used in this study. In the present study, infill walls are modelled as equivalent diagonal single strut in both diagonals of each bay. In order to model the strength and stiffness degradation of the infill walls in the time history analysis, pinching material model is used, which is implemented in Opensees by Ibarra et al. (2005). Pinching material model is used for hysteretic modelling of infill walls by many studies (Landi et al., 012, Ravichandran and Klinger, 2012, Nelson, 2016, etc). The Fig. 3 shows the typical force-displacement relationship of the pinching material model along with its parameters. As the equivalent strut is modelled only for compression, the capacities in tension are assumed to be very small values in order to avoid the numerical instabilities.

K_e	= Initial elastic stiffness
F_y	= Yield strength
α_h	= Isotropic hardening ratio
R	= Residual stress ratio
α_{cap}	= Slope of the post capping branch as a fraction of initial stiffness
α_{cap}	= Slope of the post capping branch as a fraction of initial stiffness

Fig. 3. Pinching material model for Infill wall

6.3 Validation study: One storey one bay RC infilled frame (Colangelo [37])

In order to validate the modelling approaches used in the present study, the pseudo-dynamic experimental test carried out by Colangelo (1999) on single storey infilled plane frame as shown in Fig. 4 is chosen for validating the computational model. The frame was tested with a pseudo-dynamic load using the E-W component of the 1976 Friulli earthquake as shown in Fig. 5. Detailed description of the test-rig, the material properties, as well as the loading regime, can be found in Biondi et al. (2000) and Seismosoft (2013). The

nonlinear pseudo-dynamic time history analysis is conducted and the base shear time histories are recorded. Fig. 6 shows the comparison between the base shear time history obtained from the experimental study and the present computational study, it can be seen that the two results match closely.
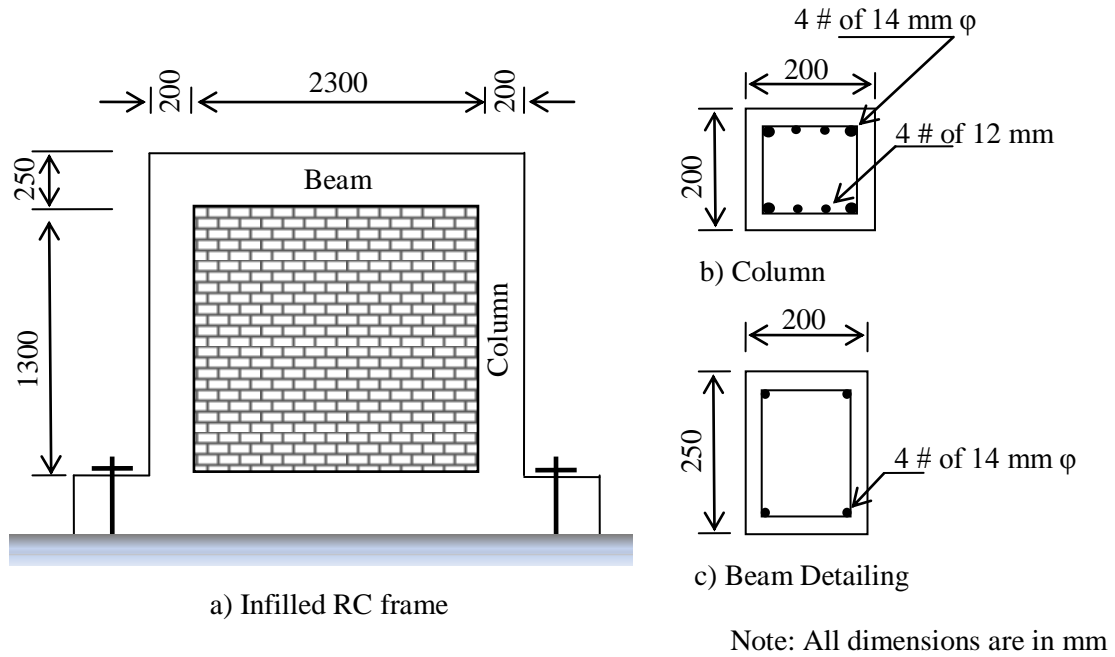

a) Infilled RC frame

b) Column

c) Beam Detailing

Note: All dimensions are in mm

Figure4. Reaction scheme of synthesis of ibuprofen derivatives through esterification reaction.
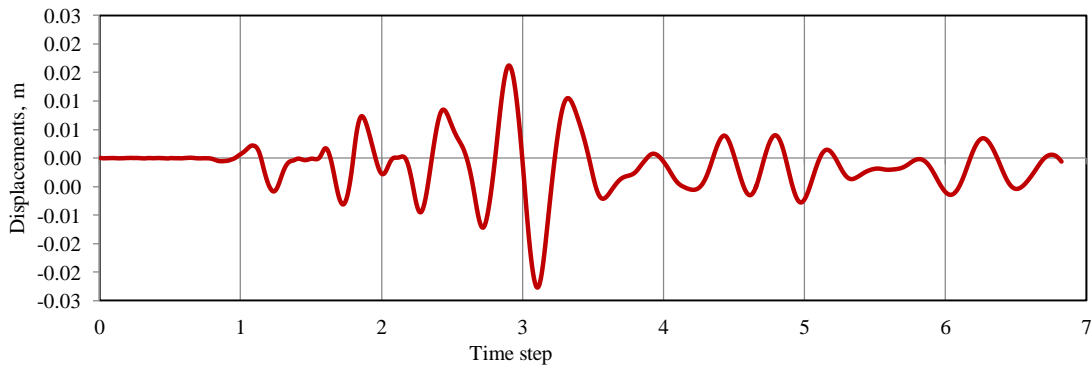

Fig. 5: Displacement history E-W component of 1976 Friulli earthquake
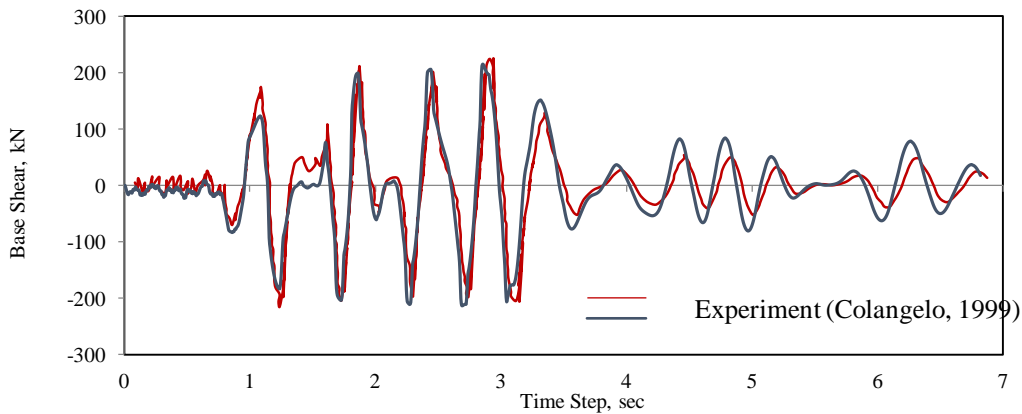

Fig. 6: Comparison of base shear histories obtained from experimental and computational study.

From this study it is clear that the computational model and the analysis procedure adopted in the present study yields the reasonably accurate behaviour of structures.

6.4 Selection of Earthquake Ground Motion

Fragility analysis requires large number of ground motion data for nonlinear dynamic analysis. Regarding the number of earthquakes required for developing fragility curves, there are no clear guidelines reported in the literature. ATC 58 (2012) recommends a suite of 11 pairs of ground motions for a reliable estimate of the response quantities. ASCE/SEI 41 (2007) suggests 30 recorded ground motions to meet the spectral matching criteria for Nuclear power plant structures. Celik and Ellingwood (2010) used 40 ground motions for developing fragility curves. As the present study is limited to Indian context, due to scarcity of data, thirteen pairs (26 ground motions) of available real ground motions with PGA ranging from 0.1g to 1.5g are selected from East Asia-India region (http://strongmotioncenter.org/). The details of the selected ground motions are shown in the Table 3.

Table 3: Selected Ground motions events and corresponding parameters

S.No	Event	Magnitude	PGA, g		Hypocentral distance (km)	Site Geology:	Location
1	Chamoli Aftershock 1999-03-29 08:49:45 UTC	4.6	0.1	0.11	24.6	Rock	Gopeshwar, India
2	Chamoli 1999-03-28 19:05:11 UTC	6.6	0.16	0.22	123.7	Rock	Barkot, India
3	Chamba 1995-03-24 11:52:33 UTC	4.9	0.24	0.29	37.5	Rock	Rakh, India
4	India-Burma Border 1995-05-06 01:59:07 UTC	6.4	0.3	0.42	261.9	Soil	Haflong, India
5	India-Burma Border 1987-05-18 01:53:51 UTC	5.9	0.46	0.39	155	Rock	Panimur, India
6	India-Burma Border 1990-01-09 18:51:29 UTC	6.1	0.55	0.6	233.5	Rock	Laisong, India
7	India-Bangladesh Border 1988-02-06 14:50:45 UTC	5.8	0.64	0.78	117.5	Rock	Khliehriat, India
8	Xizang-India Border 1996-03-26 08:30:25 UTC	4.8	0.76	0.37	49.9	Rock	Ukhimath, India
9	NE India 1986-09-10 07:50:26 UTC	4.5	0.88	0.87	50.9	Rock	Dauki, India
10	India-Burma Border 1988-08-06 00:36:25 UTC	7.2	0.96	0.9	206.5	Rock	Hajadisa, India
111	Bhuj/Kachchh 2001-01-26 03:16:40 UTC	7.0	1.03	0.9	239	-	Ahmedabad, India
12	Uttarkashi 1991-10-19 21:23:15 UTC	7.0	1.15	1.16	39.3	Rock	Ghansiali, India
13	India-Burma Border 1997-05-08 02:53:15 UTC	5.6	1.48	0.93	65.4	Soil	Silchar, India

6.5 Material uncertainty

Material properties of concrete, steel and infill walls used in the construction are random in nature. It is important to incorporate the uncertainties in all possible material and modelling parameters in the computational model to have a more realistic representation of the responses in a probabilistic assessment. For Indian conditions, Ranganathan (1999) studied the randomness in the strength of concrete and steel and proposed normal distributions for these properties with statistical parameters presented in Table 5. Similarly statistical parameters required for properties of infill walls are adopted from Agarwal and Thakkar (2001) as shown Table 4. Thickness of a masonry wall in this study is considered as 230 mm which is the thickness commonly found in

Indian construction practice. Young's Modulus of a masonry wall is taken as 2300 N/mm2 (Kaushik et al. , 2007).

It is reported in many studies (Celik and Ellingwood (2010); Davenport and Carroll (1986), etc) that damping can be random in nature. Randomness in damping is considered in the present study. The mean value of global damping for RC buildings is considered as 5%, as suggested by IS 1893 (2002). Damping is modelled as per Rayleigh damping with COV of 40% as suggested by Davenport and Carroll (1986). A set of 26 values for each random variable are generated using Latin Hypercube Sampling as 26 models are considered in developing fragility curves.

Table 4: Details of random variables used in LHS scheme

Material/Property	Variable	Mean	COV (%)	Distribution	Remarks
Concrete	fck	30.28 MPa	21.0	Normal	Uncorrelated
Steel	fy	468.90 MPa	10.0	Normal	Uncorrelated
Global Damping ratio	ξ	5%	40.0	Normal	Uncorrelated
Masonry (Shear Strength)	τc	0.204 MPa	12.0	Normal	Uncorrelated

VII. PROBABILISTIC SEISMIC DEMAND MODEL (PSDM)

The 26 natural ground motions are selected such the PGAs of the ground motions are ranging from 0.1g to 1.48g. Based on LHS scheme, 26 computational models are developed and each model is analysed for a particular ground motion (randomly selected). A total of 26 nonlinear dynamic time history analyses are performed and the maximum inter-storey displacement (EDP) for each storey are monitored. The maximum storey displacements at each storey along with the corresponding PGAs (IM) are recorded and plotted in logarithmic graph. A power law (refer Eq. 6) relationship for each storey is fitted using regression analysis, which represents the PSDM model for that storey. Out of all PSDM models for each storey levels for a particular frame, the PSDM model that produce maximum inter-storey drift is considered as the governing PSDM model. A power law (refer Eq. 6) relationship for each frame is fitted using regression analysis, which represents the PSDM model for the corresponding frames. Fig. 7 shows the governing PSDM models for all the frames considered.

The regression coefficients a and b for each governing PSDM model for all frames, along with corresponding R2 value are reported in Table 5. The PSDM model provides the most likely value of inter-storey drift (in percentage) in the event of an earthquake of certain PGA (up to 1.48g) in each frame. Depending on the values of parameters 'a & b', the vulnerability of the particular frame can be identified. It can be seen from Fig. 13 that, the percentage drift for any given PGA is the highest for the partially infilled frames, which shows that these frame are likely to be more vulnerable. It can also be seen that at smaller PGA values, the inter-storey drifts for fully infilled frames are less than that of bare frames. At a PGA value of higher than 0.8g the inter-storey drifts of infilled frame becomes almost equal to that of bare frame. This may be due to the fact that at higher PGA values the infill walls loses its strength and behaves like a bare frame.
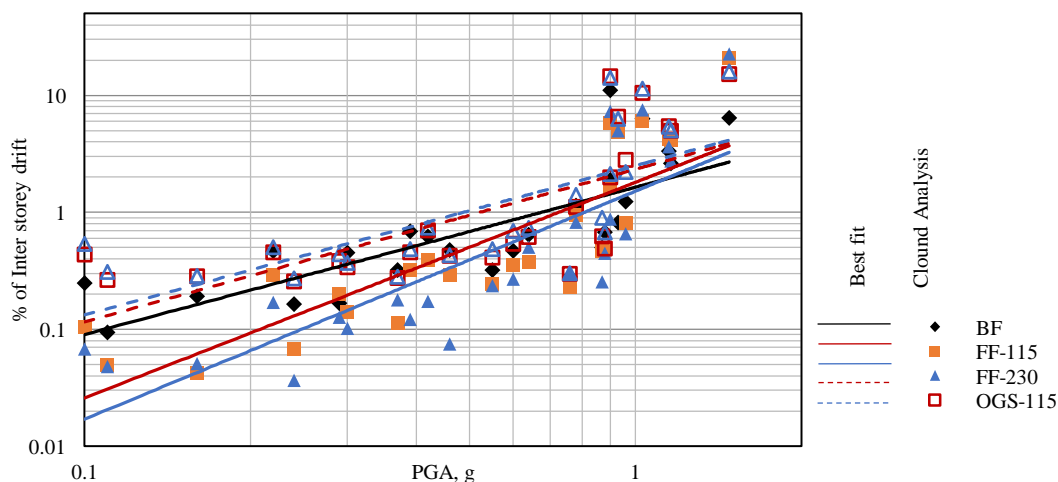

Fig. 7: Probabilistic Seismic demand model for frames considered

Table 5: Regression coefficients a and b and corresponding R2 from PSDM model

Frame Configuration	a	b	R2
Bare Frame (BF)	1.639	1.259	0.59
Fully Infilled Frame	1.805	1.844	0.70
Fully Infilled Frame	1.516	1.949	0.68
Partially Infilled frame	2.334	1.304	0.51
Partially Infilled frame	2.506	1.277	0.52

VIII.   FRAGILITY CURVES

The dispersions of inter-storey drifts $\beta_{D/IM}$ is calculated using the Eq. 9. The dispersion component $\beta comp$ is found out using Eq. 8. In order to study the effect of different infill wall thickness on the probability of being in or exceedance of each damage limit state (S_c), the fragility curves are developed (Eq. 7) for all the frames from the governing PSDM models. Fig. 8 shows the governing fragility curves for each frame for different performance levels namely, IO, LS and CP. It can be seen that the fully infilled frames having 230 mm wall thickness display low probability of exceedance followed by fully infilled frames having 115mm wall thickness. Partial infilled frames show higher exceedance probability indicating that they are more vulnerable.

a) Immediate Occupancy (IO)   b) Life Safety (LS)

c) Collapse Prevention (CP)
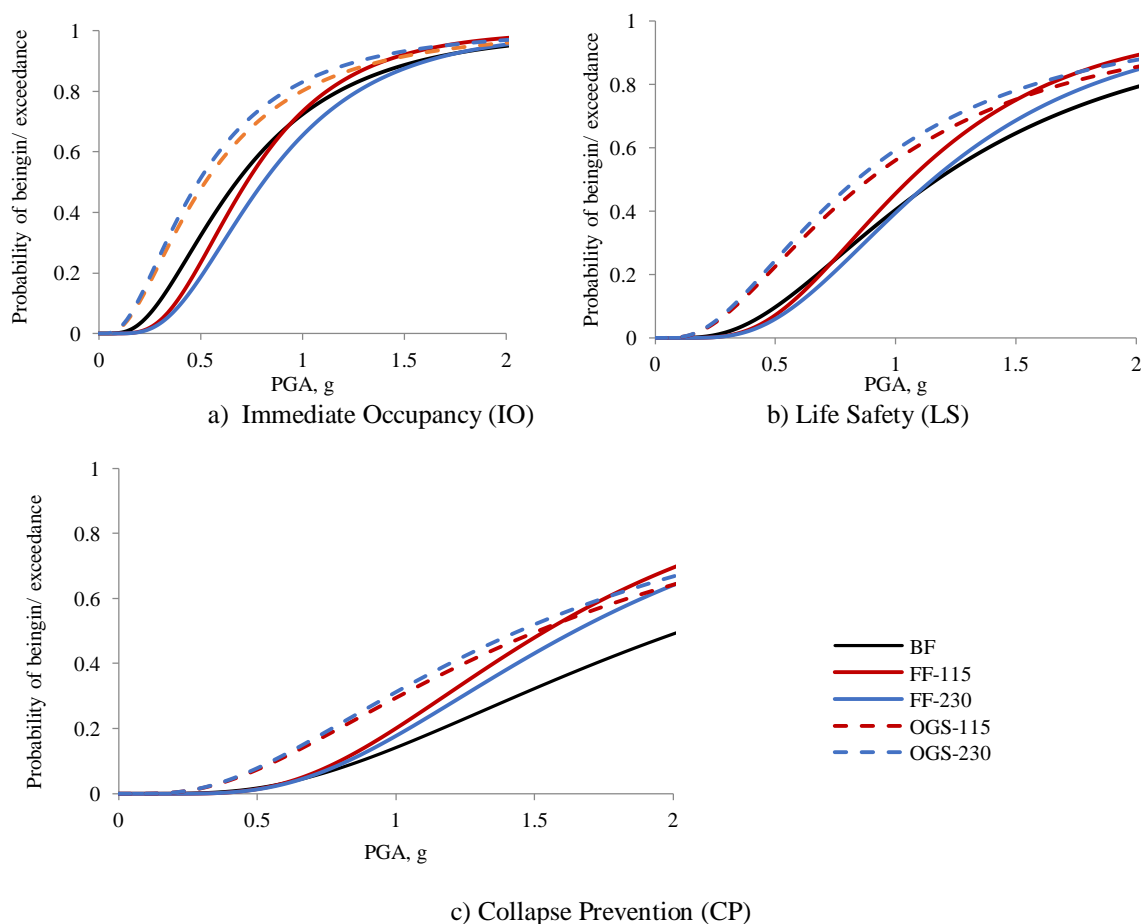
Fig. 8: Fragility curves for the frames considered for Immediate Occupancy performance limit state

IX. RELIABILITY CURVES

In order to understand the relative performance of each frame quantitatively, seismic reliability indices are calculated. The reliability indices are estimated by combining (using the Eq. 2) the fragility curves for each storey for particular limit states with a seismic hazard curve. In the present study, hazard curve (Fig. 1) of North East India is chosen for reliability index estimation.

Reliability indices for each storey for all the frames are calculated for two performance objectives, namely (i) life safety for an earthquake having 10% probability of occurrence in 50 years (Performance

objective I) and (ii) collapse prevention for an earthquake having 2% probability of occurrence in 50 years (Performance objective II). The calculated reliability indices for each storeys are presented in the Table 6.

9.1. Storey wise reliability indices for Performance objective I

Fig. 14 shows storey wise reliability index values for all the frames graphically. The reliability index of the bare frame for performance objective I is ranging from 2.70 – 3.39. The lowest value of reliability index is found to be 2.70 which corresponds to the predominantly high inter-storey drift at second storey level. Similarly, for fully and partially infilled frames the lowest value of the reliability indices are governed by first storey. The storey wise variation of reliability index values for fully infilled frames is almost linear. Whereas, for the partially infilled frames, the reliability index values for the upper storeys are very high as compared to first storey and the variation of reliability index across the storeys follow a nonlinear trend. In fact, for an efficient design variation of reliability index should follow a uniform trend across the storeys.

9.2 Fully infilled frames for Performance objective I

Governing reliability index for fully infilled frame having wall thickness of 230mm (βpf = 2.85) is found to be higher than that of frames having 115mm wall thickness. The reliability index is found to be higher in all storeys of frame with 230mm wall than that of 115mm wall. This shows that, if the infill walls are uniformly distributed in all storeys, as the thickness of infill wall increases the global performance of the structure also increases. This behaviour is reversed in the case of partially infilled frames.

9.3 Partially infilled frames for Performance objective I

The governing reliability index for partially infilled frame having infill wall thickness of 230 mm (β_{pf} = 2.32) is lower than that of 115mm (β_{pf} = 2.35). It is found that the reliability index for upper storeys of partially infilled frames with 230mm walls are much higher than the corresponding values for frames with 115mm walls. This shows that frames with 230mm walls are more rigid in the upper storeys and makes the first storey as more vulnerable as compared to that of frames with 115mm wall. This shows that, if the frame is partially infilled, as the thickness of infill wall increases the global performance of the structure decreases. Similar kind of conclusions can be drawn for the performance objective II. The dispersions of inter-storey drifts $\beta_{D/IM}$ is calculated using the Eq. 9. The dispersion component $\beta comp$ is found out using Eq. 8. In order to study the effect of different infill wall thickness on the probability of being in or exceedance of each damage limit state (Sc), the fragility curves are developed (Eq. 7) for all the frames from the governing PSDM models. Fig. 8 shows the governing fragility curves for each frame for different performance levels namely, IO, LS and CP. It can be seen that the fully infilled frames having 230 mm wall thickness display low probability of exceedance followed by fully infilled frames having

Table 6: Reliability Index (β_{pf}) for all frames (inter-storey drift of each storey as EDP)

Frame Configurations	Storey Level							
	Performance objective I				Performance objective II			
	1st	2nd	3rd	4th	1st	2nd	3rd	4th
Bare Frame (BF)	2.78	2.70	3.09	3.39	3.21	3.15	3.74	4.20
Fully Infilled Frame (115 mm Thick wall)	2.80	3.06	3.74	4.27	3.12	3.48	4.43	5.03
Fully Infilled Frame (230 mm Thick wall)	2.85	3.54	4.30	5.14	3.15	4.05	5.07	6.08
Partially Infilled frame (115 mm Thick wall)	2.35	4.28	5.28	5.20	2.73	4.94	6.05	5.91
Partially Infilled frame (230mm Thick wall)	2.32	6.59	7.50	8.21	2.71	7.46	8.51	9.37

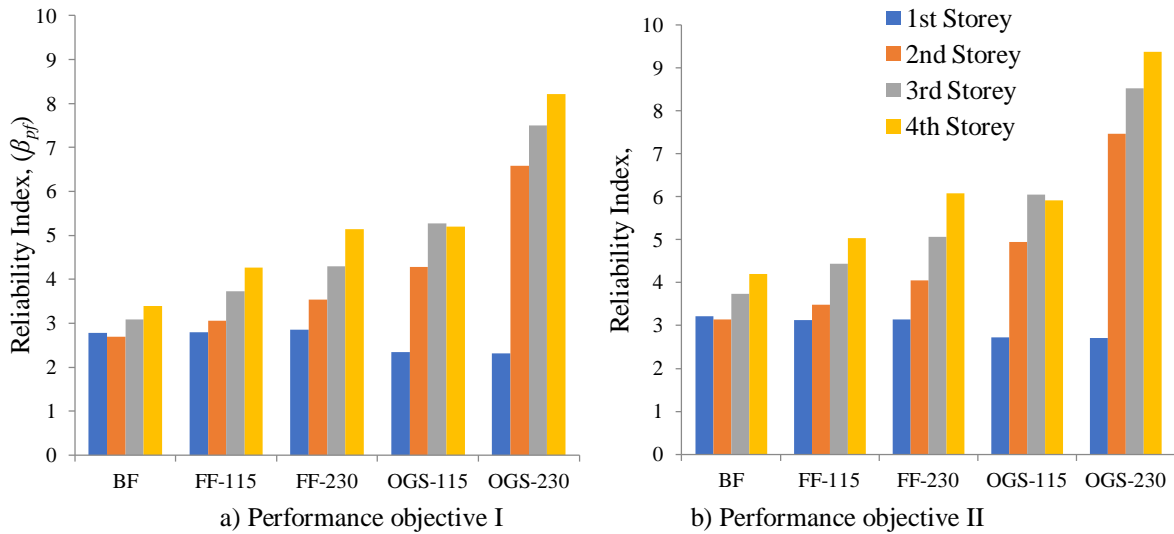a) Performance objective I   b) Performance objective II

Fig. 14: Storey wise comparison of Reliability Index (β_{pf}) for all frames

X. CONCLUSIONS

The performance comparison of bare frames, fully infilled frames and partially infilled frames is not explored focussing on different infill wall thickness in probabilistic frame work so far. In order to study the effect of infill walls having different thickness in a framed building, various frames such as bare, fully infilled and partially infilled frames are considered. PSDM and Fragility curves are developed for the frames as per SAC-FEMA method and corresponding reliability index values are estimated for two performance objectives.

- At smaller PGA values the fully infilled frames are stiffer than bare frames but at higher PGAs infill walls fail and behave like a bare frame. This behaviour is observed from the PSDM model.
- Partial infilled frames are found to be more vulnerable than fully infilled frames as reported by past studies.
- Increasing the thickness of infill wall is beneficial to the global performance of buildings for a fully infilled frame and detrimental for partially infilled frames. Increase in the infill wall thickness always guaranty the better performance in the case of frames with uniformly infilled in all storeys.
- When the infill wall thickness in a partially infilled frame decreases, the vulnerability of the frame reduces. However, partially infilled frames are not recommended due to the extremely low stiffness/strength in the first storey.
- The reliability index variation should follow a uniform trend ideally for an efficient design. Due to many practical reasons it is seldom possible. However, a linear variation of reliability index across the storeys can be an acceptable choice. This trend is observed in fully infilled frames. Whereas a partially infilled frames shows a different trend far away from this linear variation.

Conflict of interest
There is no conflict to disclose.

REFERENCES

[1]. Agarwal P. and Thakkar S.K., 2001. A comparative study of Brick masonry house model under Quasi-Static and dynamic loading. Journal of Earthquake Technology, 38 (2-4), 103-122.
[2]. Al-Chaar, G., 2002. Evaluating strength and stiffness of unreinforced masonry infill structures. US Army Corp of Engineers, Engineer Research and Development Center.
[3]. Anil, O. and Altin, S., 2007. An experimental study on reinforced concrete partially infilled Frames. Engineering Structures, 29, . 449–460.
[4]. ASCE/SEI 41-06, 2007. Seismic Rehabilitation of Existing Buildings. American Society of Civil Engineers. USA.
[5]. ATC 58 100% Draft, 2012. Guidelines for Seismic Performance Assessment of Buildings. Applied Technology Council, Redwood City, CA
[6]. Avinash Karthick, M. Sriraman, Nelson Ponnu Durai, D.C. Haran Pragalath, (2017). Fragility curves by sac fema and ann method, International Journal of Civil Engineering and Technology, 8(7), 1103 -1110.
[7]. Biondi S, Colangelo F, Nuti C, 2000. La Risposta Sismica dei Telai con Tamponature Muraie, (in Italian). Gruppo Nazionale per la Difesa dai Terremoti, Rome.
[8]. Buonopane, S. and White, R.,1999. Pseudodynamic testing of masonry infilled reinforced concrete frame. Journal of Structural Engineering, 125, 578–589.
[9]. Celarec D., Ricci P. and Dolsek M., 2012. The sensitivity of seismic response parameters to the uncertain modeling variables of masonry-infilled reinforced concrete frames. Engineering Structures. 35, 165–177.
[10]. Celik, O. C. and Ellingwood B. R., 2010. Seismic fragilities for non-ductile reinforced concrete frames-role of aleatoric and

epistemic uncertainties, Structural Safety. Vol.32, pp. 1-12.

[11]. Colangelo F, 1999. Qualificazione, Risposta Sismica Pseudodinamica e Modelli Fenomenologici di Portali di C.A.Tamponati con Laterizio, (in Italian). DISAT, Italy.

[12]. Cornell, C. A., F. Jalayer, R. O. Hamburger and D.A. Foutch., 2002. The probabilistic basis for the 2000 SAC/FEMA steel moment frame guidelines. Journal of Structural Engineering, 128(4), 526-533.

[13]. Davenport, A. G. and Carroll, H., 1986. Damping in tall buildings: its variability and treatment in design, ASCE Spring Convention, Seattle, USA, Building Motion in wind, 42-57.

[14]. Davis P. R., Padhy K. T, Menon D. and Prasad. A. M., 2010. Seismic fragility of open ground storey buildings in India, 9th US National and 10th Canadian Conference on Earthquake Engineering, Toronto, Paper #. 926.

[15]. Dolsek M. and Fajfar P., 2008. The effect of masonry infills on the seismic response of a four-storey reinforced concrete frame – a deterministic assessment. Engineering Structures. 30(7),1991–2001.

[16]. Ellingwood, B. R., 2001. Earthquake risk assessment of building structures. Reliability Engineering and System Safety, 74,251-262.

[17]. Frank McKenna, Christopher McGann, Pedro Arduino and Joseph Allen Harmon, 2014. OpenSees Laboratory, https://nees.org/resources/openseeslab.

[18]. Ghobarah A., 2000. Performance-based design in earthquake engineering: state of development. Engineering Structures. 23, 878-884.

[19]. Hashemi, A. and Mosalam, K.M., 2006. Shake-table experiment on reinforced concrete structure containing masonry infill wall. Earthquake Engineering & Structural Dynamics, 35, 1827–1852.

[20]. Haran Pragalath DC, Avadhoot B, Robin DP, Pradip S, 2015a Multiplication factor for open ground storey buildings–a reliability based evaluation, Earthquake Engineering and Engineering Vibration, 15 (2), 283-295.

[21]. Haran Pragalath D C, R. Davis, P.Sarkar, 2015b. Reliability evaluation of RC frame by two major fragility analysis methods, Asian journal of civil engineering, 16(1) 47-66.

[22]. Holmes, M., 1961. Steel frame with brickwork and concrete infilling. ICE Proceedings, 19, 473–478.

[23]. Ibarra, L. F., Medina, A., and Krawinkler, H., 2005. Hysteretic models that incorporate strength and stiffness deterioration. Earthquake Engineering and Structural Dynamics. 34, 1489-1511.

[24]. IS 1893 Part I, 2002. Indian standard criteria for earthquake resistant design of structures. Bureau of Indian Standards. New Delhi.

[25]. IS 456., 2000. Indian standard for plain and reinforced concrete code of practice. Bureau of Indian Standards, New Delhi.

[26]. IS 13920, 1993. Ductile detailing of reinforced concrete structures subjected to seismic forces - code of practice. Bureau of Indian Standards, New Delhi.

[27]. Kaltakci, M. Y, Koken, A. and Korkmaz, H. H., 2008. An experimental study on the behavior of infilled steel frames under reversed-cycling loading. Iranian Journal of Science & Technology, Transaction B, Engineering, 32, 157-160.

[28]. Kaushik, H. B. Rai, D. C. and Jain, S. K., 2007 Stress-strain characteristics of clay brick masonry under uniaxial compression. Journal of Materials in Civil Engineering. 19(9), 728-239.

[29]. Kent, D. and Park, R., 1971. Flexural mechanics with confined concrete. Journal of the Structural Division, Proceedings of ASCE, ST7,. 1969-1990 .

[30]. Kunnath. S. K., 2007,. Application of the PEER PBEE methodology to the I-880 viaduct, Pacific Earthquake Engineering Research Center, University of California, Berkeley.

[31]. Landi, L. Diotallevi. P. P. and Tardini, A., 2012. Calibration of an equivalent strut model for the nonlinear seismic analysis of infilled RC frames. 15th World Conference on Earthquake Engineering, Lisboa, Portugal.

[32]. Lee, H. S. and Woo, S.-W., 2002. Effect of masonry infills on seismic performance of a 3-storey R/C frame with non-seismic detailing. Earthquake Engineering & Structural Dynamics. 31, 353–378.

[33]. Lee T. H. and Mosalam K. M., 2004. Probabilistic fiber element modeling of reinforced concrete structures, Computers and Structures. 82, 2285-2299.

[34]. Mainstone, R.J., 1971. On the stifness and strengths of infilled frames. ICE Proceedings, 230.

[35]. Mainstone, R.J. and Weeks, G.A., 1970. The influence of a bounding frame on the racking stiffness and strengths of brick walls. SIBMAC Proceeding. Presented at the Second International Brick Masonry Conference, Building Research Station, England.

[36]. Mehrabi, A.B., Benson Shing, P., Schuller, M.P., Noland, J.L., 1996. Experimental evaluation of masonry-infilled RC frames. Journal of Structural Engineering, 122, 228–237.

[37]. Mosalam, K. M., Ayala, G., White, R. N. and Roth, C., 1997. Seismic fragility of LRC frames with and without masonry infill walls. Journal of Earthquake Engineering, 1(4), 693-720.

[38]. Nelson Ponnu Durai, J Arunachalam, L Avinash Karthich, DC Haran Pragalath, D Iswarya, Robert Singh, 2016, ,Computational model for infill walls under cyclic loads, International Journal of Applied Engineering Research, 11(4) 2786-2790

[39]. Nielson, B. G., 2005. Analytical fragility curves for highway bridges in moderate seismic zones, Ph.D. Thesis, Georgia Institute of Technology.

[40]. Pallav, K., Raghukanth, S. T. G. and Singh, K. D., 2012. Probabilistic seismic hazard estimation of Manipur, India, Journal of Geophysics and Engineering. 9, 516–533.

[41]. Panagiotakos T. B. and Fardis M. N., 1996. Seismic response of infilled RC frame structures. Proceedings of the 11th world conference on earthquake engineering.

[42]. Polyakov, S.V., 1960. On the interaction between masonry filler walls and enclosing frame when loaded in the plane of the wall, in construction in seismic regions. Translation in Earthquake Engineering, Earthquake Engineering Research Institute, Moscow,. 36–42.

[43]. Rajeev, P. and Tesfamariam, S., 2012. Seismic fragilities for reinforced concrete buildings with consideration of irregularities. Structural Safety. 39,1-3.

[44]. Ranganathan, R., 1999. Structural reliability analysis and design. Jaico Publishing House, Mumbai.

[45]. Ravichandran, S. S. and Klinger, E. R., 2012. Seismic design factors for steel moment frames with masonry infills: Part I, Earthquake Spectra. 28(3), 1189-1204.

[46]. Seismosoft, 2013. SeismoStruct v6.0 - Verification Report. Available from URL: www.seismosoft.com.

[47]. Stafford-Smith, B., 1962. Lateral stiffness of infilled frames. Journal of Structural Division, 88, 183–199.

[48]. Song, J. and Ellingwood, B. R., 1999. Seismic reliability of special moment steel frames with welded connections: II. Journal of Structural Engineering, 125(4), 372.